

**Dieses Dokument ist eine Zweitveröffentlichung (Verlagsversion) /  
This is a self-archiving document (published version):**

U. Marschner, E. Starke, J.-H. Yoo, A. B. Flatau

**Improved equivalent circuit modeling and simulation of  
magnetostrictive tuning fork gyro sensors**

**Erstveröffentlichung in / First published in:**

*SPIE Smart Structures and Materials + Nondestructive Evaluation and  
Health Monitoring*. Portland, 2017. Bellingham: SPIE, Vol. 10168 {Zugriff am: 23.05.2019}.

DOI: <https://doi.org/10.1117/12.2263973>

Diese Version ist verfügbar / This version is available on:

<https://nbn-resolving.org/urn:nbn:de:bsz:14-qucosa2-351369>

„Dieser Beitrag ist mit Zustimmung des Rechteinhabers aufgrund einer (DFGgeförderten) Allianz- bzw. Nationallizenz frei zugänglich.“

This publication is openly accessible with the permission of the copyright owner. The permission is granted within a nationwide license, supported by the German Research Foundation (abbr. in German DFG).

[www.nationallizenzen.de/](http://www.nationallizenzen.de/)

# PROCEEDINGS OF SPIE

[SPIDigitalLibrary.org/conference-proceedings-of-spie](https://www.spiedigitallibrary.org/conference-proceedings-of-spie)

## Improved equivalent circuit modeling and simulation of magnetostrictive tuning fork gyro sensors

U. Marschner, E. Starke, J.-H. Yoo, A. B. Flatau

U. Marschner, E. Starke, J.-H. Yoo, A. B. Flatau, "Improved equivalent circuit modeling and simulation of magnetostrictive tuning fork gyro sensors," Proc. SPIE 10168, Sensors and Smart Structures Technologies for Civil, Mechanical, and Aerospace Systems 2017, 101681F (12 April 2017); doi: 10.1117/12.2263973

**SPIE.**

Event: SPIE Smart Structures and Materials + Nondestructive Evaluation and Health Monitoring, 2017, Portland, Oregon, United States

# Improved equivalent circuit modeling and simulation of magnetostrictive tuning fork gyro sensors

U. Marschner<sup>a</sup>, E. Starke<sup>a</sup>, J.-H. Yoo<sup>b</sup>, and A.B. Flatau<sup>b</sup>

<sup>a</sup> Institute for Semiconductor and Microsystems Technology, Technische Universität Dresden, 01062 Dresden, Germany; <sup>b</sup> University of Maryland, Department of Aerospace Engineering, College Park, MD, U.S.A.

## ABSTRACT

In this paper a new equivalent circuit is presented which describes the dynamics of a prototype micro-gyro sensor. The concept takes advantage of the principles employed in vibratory gyro sensors and the ductile attributes of GalFeNOL to target high sensitivity and shock tolerance. The sensor is designed as a tuning fork structure. A GalFeNOL patch attached to the y-z surface of the drive prong causes both prongs to bending the x-z plane (about the y axis) and a patch attached to the x-z surface of the sensing prong detects Coriolis-force induced bending in the y-z plane (about the x axis). A permanent magnet is bonded on top of each prong to give bias magnetic fields. A solenoid coil surrounding the drive prong is used to produce bending in the x-z plane of both prongs. The sensing prong is surrounded by a solenoid coil with N turns in which a voltage proportional to the time rate of change of magnetic flux is induced.

The equivalent circuit enables the efficient modeling of a gyro sensor and an electromechanical behavioral simulation using the circuit simulator SPICE. The prongs are modeled as wave guiding bending beams which are coupled to the electromagnetic solenoid coil transducer. In contrast to known network approaches, the proposed equivalent circuit is the first tuning fork model, which takes full account of the fictitious force in a constant rotating frame of reference. The Coriolis force as well as the centrifugal force on a concentrated mass are considered.

**Keywords:** Tuning fork gyro sensor, Coriolis force network model, Galfenol, Dynamic bending beam model, Mode shapes, Wave guide

## 1. INTRODUCTION

Miniaturized gyro sensors are a substantial component of many applications where rotational velocity is processed. For example, gyro sensors are needed in an electronic stability program (ESP) to detect loss of steering control, in hand held devices to determine their rotational movement, in robotics and spacecrafts for orientation determinations and forecasts, or in still cameras for image stabilization. Various gyro sensor configurations exist, for example accelerometers with silicon-glass structure, butterfly shaped gyroscopes, beam structures or tuning fork structures [1-4].

In order to study the ductile attributes of GalFeNOL to target high sensitivity and shock tolerance in a meso-scale gyro sensor numerically and experimentally, a tuning fork structures was chosen and preliminary test results were presented as concept verification by Yoo et al. [5]. Bending modes, resonant frequencies and the magnetic field distribution were computed with a finite element model (FEM) as basis for a second, improved design. This design was analyzed in [6] with an electromechanical network model or equivalent circuit, too. The equivalent circuit enabled a better understanding and explanation of the behavior of this system, which involves different physical domains, as well as fast numerical calculations, e.g. with pSpice. Experiments confirmed the predicted sidebands of the sinusoidal angular velocity.

In the previous approach, an additional force source was applied in the network model to account for the Coriolis force. The centrifugal force was neglected since a general circuit model, which accounts for both, Coriolis and centrifugal force, had not been available [7]. A new interpretation of the force balance of a vibrating point mass within a rotating frame of reference as Kirchhoff's laws lead to an equivalent circuit which takes full account of the fictitious force [8]. In the new equivalent circuit Coriolis force and Centrifugal Force are coupled by a reversible transducer. A big advantage of this model is, that it can be used without any further knowledge about the fictitious force. In this paper this new transducer model is applied to modeling and behavioral simulation of the magnetostrictive tuning fork gyro sensor. The

resulting multi-physics equivalent circuit covers two translational and rotational domains, which describe the bending prongs, the electrical domain, the Coriolis/Centrifugal force transducer as well as the magnetostrictive transducer.

The paper is structured as follows: In section 2 the advantages of network modeling the gyro sensor are discussed demonstrated in the light of different system abstraction levels. Afterwards the network model is deduced in section 3. In section 4 simulation results, obtained with the circuit simulator LTSPICE, are presented. Finally, a summary and an outlook are given in Section 5.

## 2. EFFICIENT DESIGN OF DYNAMIC SYSTEMS

Sensor modeling with electromechanical networks offers several advantages. Especially for electrical engineers it enables the very efficient simulation of different physical domains within one model [9]. In addition to models with short computing time and sufficient accuracy the understanding of interrelationships and interactions between the physical domains is a central benefit of electromechanical networks.

Multi-physics systems with a large number of components have been successfully modeled and designed by introducing a model hierarchy. As depicted in Fig. 1, a system can be typically partitioned into the four levels. The lowest level is the process/technology level. Individual production processes are characterized by process parameters. The process parameters affect the geometry and material parameters of system elements. An element may be created on process and technology level virtually applying a process or technology simulator. The element level includes function and form elements such as resistors or bending beams. Several elements form a system component. Typical elements and components are described in two and three dimensions with partial differential equations (PDE's) and boundary

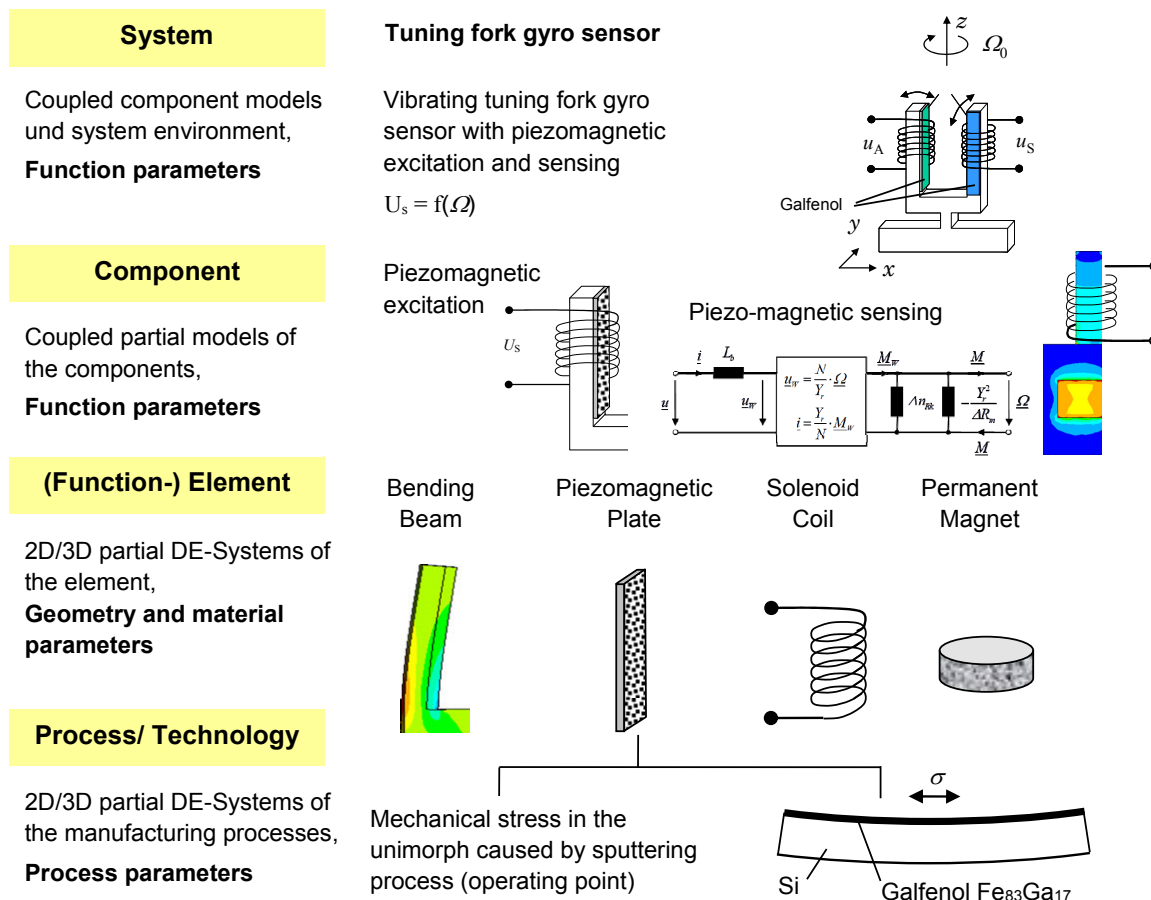


Fig. 1. Model hierarchy of the vibrating tuning fork gyro sensor with piezomagnetic excitation and sensing.

conditions, which include geometric and material parameters. Accordingly, a high computational and simulation effort results. At system level the system is described by a qualitative model structurally and/or functionally over its interfaces at a high abstract level. The description is made with the aim of a behavioral simulation at system level to check virtually, whether the design meets the system specification. The lower levels comprise more detail than the higher levels. Higher system levels are characterized by higher abstraction. Such an information compression, which lowers the precision of the simulated dynamic behavior only insignificantly, can be achieved with network modeling. Physical phenomena, like bending moments or an electrical capacitance are condensed in lumped parameters.

In Fig. 1 several partial models of a vibrating tuning fork gyro sensor are assigned to these levels of hierarchy. On each arm, but perpendicular to each other, a piezomagnetic plate is placed and both arms are surrounded by a coil. One arm is used as actuator to generate a fork vibration by application of an AC magnetic field. In case of a rotation about the yaw axis, the arm vibration perpendicular to the excited direction is caused by Coriolis force. The arm vibration is transferred into a fluctuation of the magnetic flux in the magnetostrictive plate, where a permanent magnet originates the magnetic field. Thus, a voltage is induced in the surrounding detection coil. At process level the sputtering determines the mechanical bias of piezomagnetic layer and thereby its material parameters. The geometry parameters of the piezomagnetic unimorph arms define the properties of the piezomagnetic transducer. Assuming an ideally uniform magnetic field within the solenoid coils a behavioral description of the electromechanical system can be derived analytically in form of a network model [10]. Its coupling with the Coriolis/Centrifugal force transducer allows a behavioral simulation of all involved integral quantities (force, velocity, voltage, current, etc.) using a circuit simulator.

During a simulation an experiment is conducted on the models. The behavior of components and the system behavior are assessed by hand on performance parameters which must lie within defined tolerance limits. Key performance parameters are, for example, the sensitivity of a sensor, its power consumption, temperature range, the output noise, but also its reliability, the extraction rate, and its costs [7].

### 3. EQUIVALENT CIRCUITS

The multi-physics electromechanical equivalent circuit consists of the dynamic bending beam models of the tuning fork prongs for excitation and sensing mode, of the Coriolis/Centrifugal force transducer and the magnetostrictive transducer. In Fig. 2 the discretization of the tuning fork to model the excitation mode is depicted. For the depicted excitation mode the prongs are modeled as bending beam with finite beam elements as in [6], each containing a concentrated mass  $\Delta m$  and a concentrated rotational compliance  $\Delta n_R$ . As boundary condition the bending of the crossbar expressed by the bending compliance  $n_{Rb}$  is assumed. At the beam end ⑤ the no-load boundary conditions  $\underline{F}_n = 0$  and  $\underline{M}_{xn} = 0$  are applied.

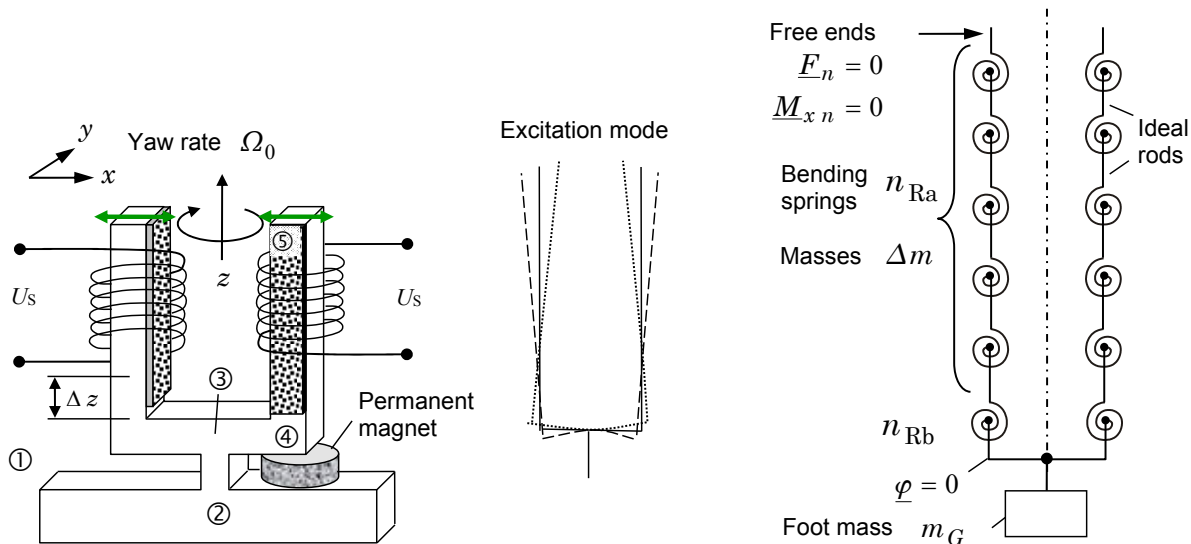


Fig. 2. Excitation mode discretization of the tuning fork

Table 1. Port (terminal) quantities of the involved physical systems

Physics	Across quantity	Through quantity
Electrical system	Voltage $u$	Electrical current $i$
Translational system	Velocity $v$	Force $F$
Rotational system	Rotational velocity $\Omega$	Moment $M$

When the physical quantities are assigned to each other as listed in Table 1, the equivalent circuit of the tuning fork excitation mode in Fig. 3 results. Rotational compliances are expressed by the inductance symbol and masses by the capacitor symbol. The transformer symbols describe the ideal rods connecting the point masses and rotational compliances [9]. Due to its symmetric shape only one half of the tuning fork including one prong needs to be modeled. In addition, the prongs can be folded down since only the vibration perpendicular to the neutral layer of the beam is of relevance. The foot mass is without influence and thus neglected. The resulting equivalent circuit describes a bending wave guide. The behavioral simulation in the frequency domain allows a quick check of the eigenfrequencies. In the time domain, moments, rotational velocities, forces and velocities at the sections can be simulated, as shown in Fig. 9.

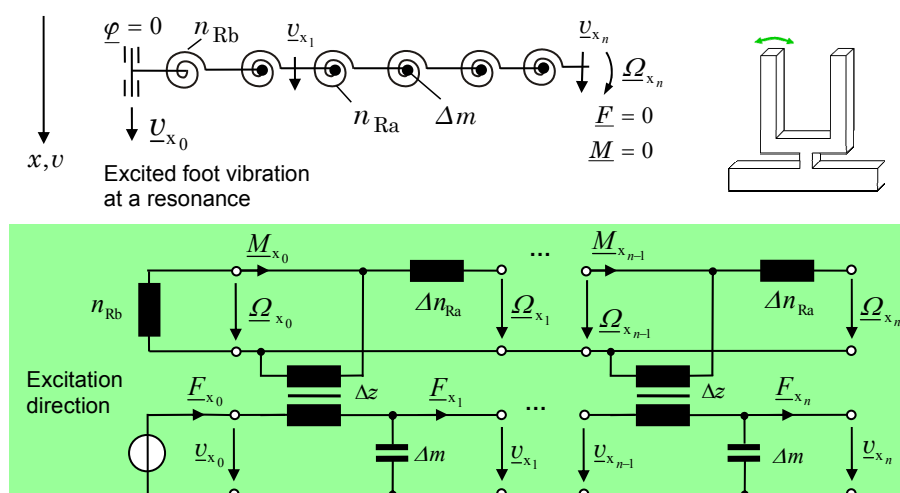


Fig. 3. Excitation mode bending waveguide equivalent circuit of the half tuning fork. The marked angular velocities are the bending angle velocities. The excitation is condensed in an ideal velocity source.

For computation of the Coriolis force the velocities of  $v_{x1}, \dots, v_{xn}$  of the beam elements in excitation direction are needed. The tuning fork is rotating in a local mechanical frame with the yaw rate  $\dot{\Omega}_0$  around the central axis, as depicted in Fig. 4. In a practical application of the gyro sensor the frequency of the dynamic vibrations of the structure is much higher than a change of the yaw rate. For this reason no moments of inertia with respect to the yaw rate and no rotational acceleration are considered. Furthermore, relative to the inertial frame of reference there is no translational movement of the frame reference or a uniform movement with a constant velocity  $\vec{v}_0$ . Based on the force balances in Fig. 5 the depicted equivalent circuit could be derived [8].

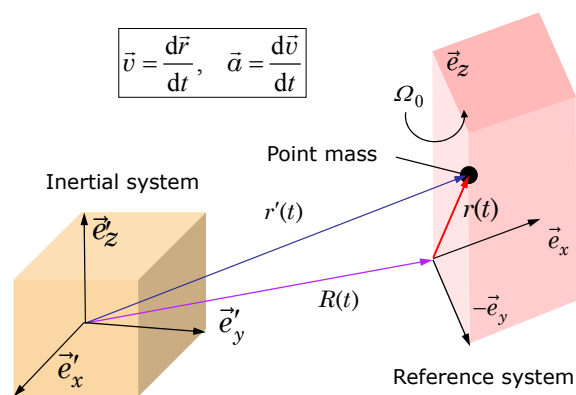


Fig. 4. Definition of the rotating frame of reference

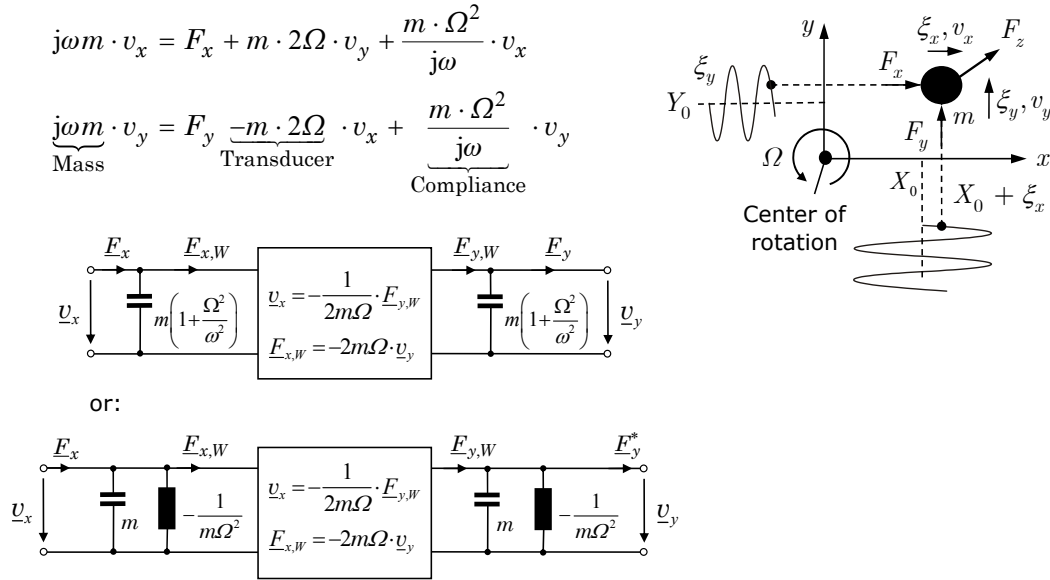


Fig. 5. Transient equivalent circuit describing a point mass in a rotating frame of reference. The mass and the compliance in the lower circuit can be combined to a frequency dependent equivalent mass in the harmonic case, represented by the upper circuit. An accelerated frame of reference or secondary rotations of elements inside the frame of reference are not covered by the model.

The network model in Fig. 5 also enables time harmonic simulations in addition to the transient modeling. In the case of harmonic vibrations the model is completely independent from the position of the point mass in the reference frame. Applying this model, the secondary vibration – perpendicular to the primary vibration and to the rotation axis – can be modeled. The magnitude of this secondary vibration is directly proportional to the angular velocity or yaw rate  $\vec{\Omega}_0$ .

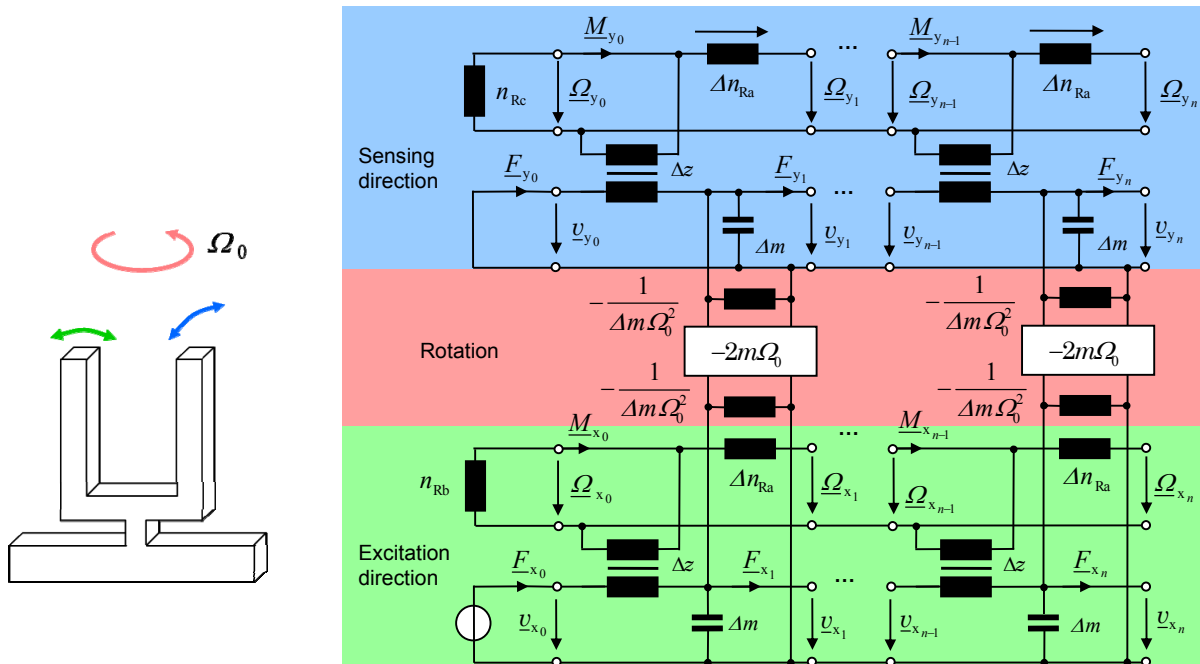


Fig. 6. Coupling of tuning fork excitation and sensing direction by the Coriolis/Centrifugal force transducer.

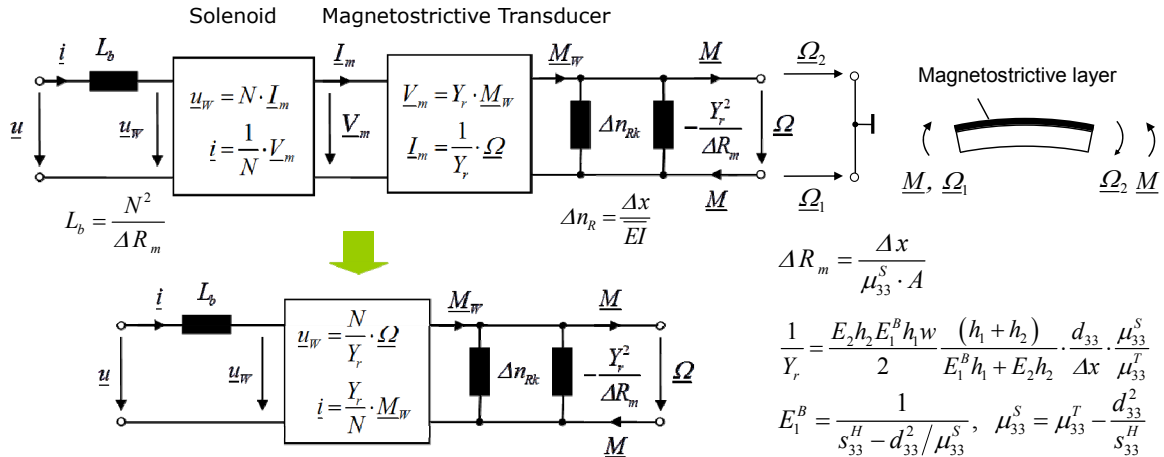


Fig. 7. Combination of the electromagnetic and the magnetostrictive transducer

In order to model the bending of the prongs perpendicular to the excitation a separate bending wave guide is required. With the exception of different bending compliances and that the crossbar between points ③ and ④ is now acting as torsional compliance  $n_{Rc}$ , the equivalent circuit in sensing direction is comparable with the excitation circuit description.

Magnetomechanical and electromagnetic coupling can be described by two reversible transducers, as derived in [10] and depicted in Fig. 7. The transduction coefficient  $Y_r$  relates moment  $M$  and magnetic voltage  $V_m$  to each other as well as rotational (bending) velocity to the magnetic flux rate. In the magnetic domain the magnetic permeance  $1/\Delta R_m$  can be measured in case of suppressed bending, that is a short cut of  $\underline{Q}$ . The compliance  $\Delta n_R$  can be measured when variations of  $\underline{V}_m$  are admitted. Both transducers can be combined to one, as demonstrated in Fig. 7.

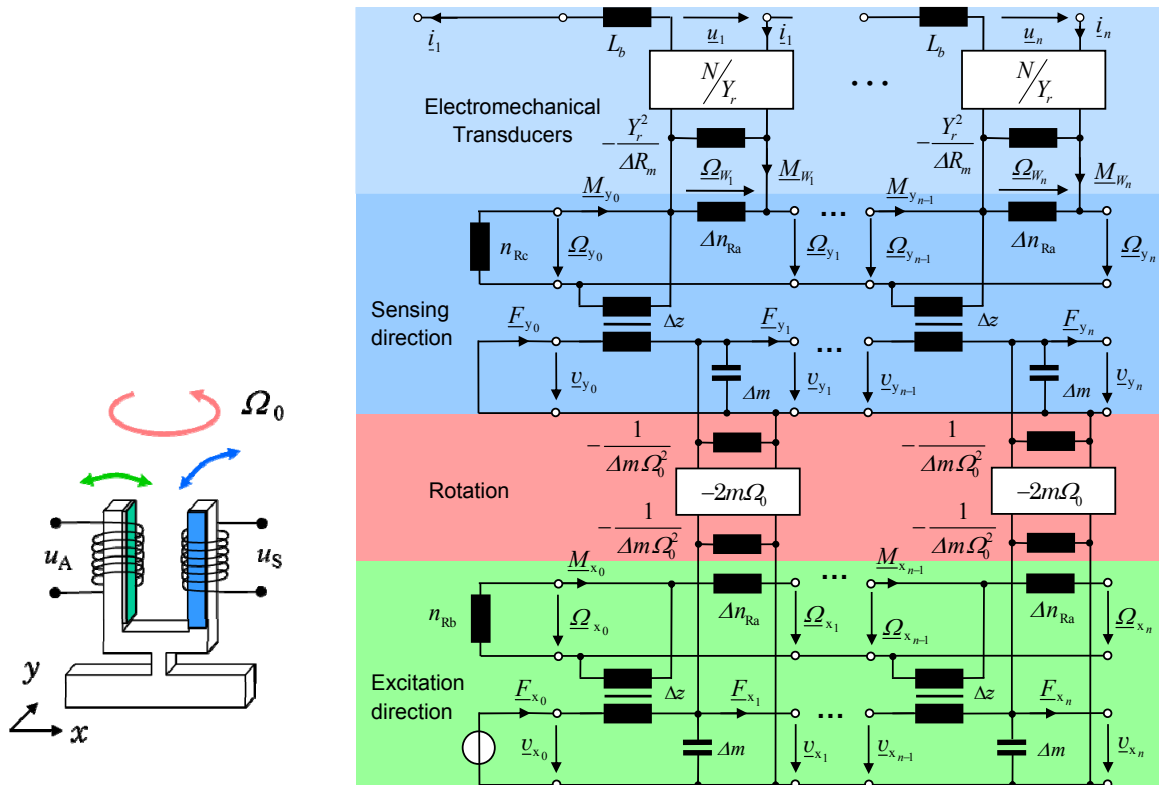


Fig. 8. Completed equivalent circuit describing the magnetostrictive tuning fork gyro sensor



Fig. 8 shows the completed equivalent circuit of the magnetostrictive tuning fork gyro sensor, where the magnetostrictive transducer was coupled with the finite bending elements of the sensing prong. The induced voltage in the sensor coil caused by the magnetic field of the drive coil and the magnetic flux variation in the sensing patch due to the vibration in excitation direction are not described by the model.

The results of a transient behavioral simulation with the circuit simulator LTSPICE are depicted in Fig. 10. The network parameters are listed in Table 2. The prong was excited at a frequency of 8.7 kHz with an arbitrary velocity of  $0.4 \mu\text{m/s}$  at its center. Different resulting physical quantities of interest at different discrete locations were displayed. When the yaw rate was increased, the sensitivity relation depicted in Fig. 10 resulted.

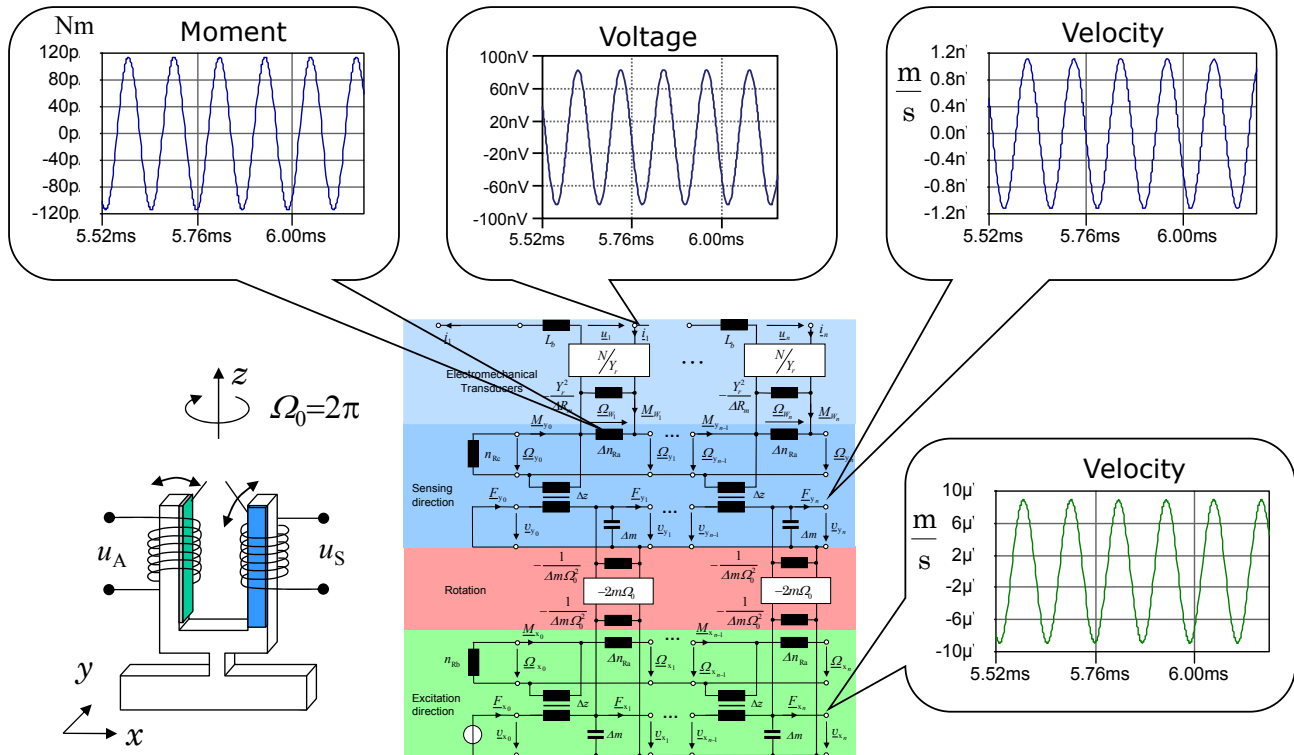


Fig. 9. LTSPICE simulation results of different physical quantities

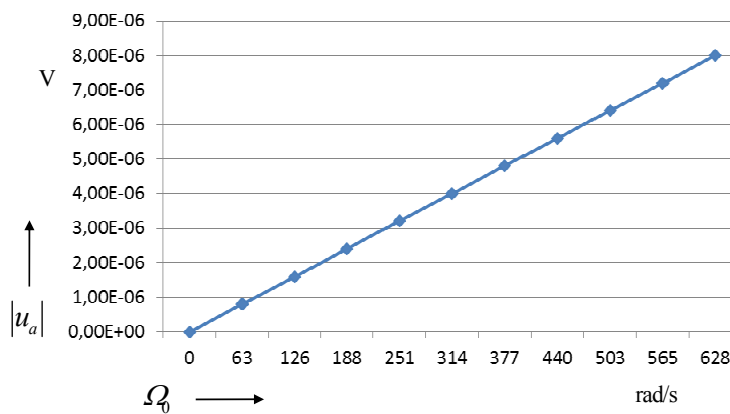


Fig. 10. LTSPICE-Simulation of the output voltage

Table 2. Simulation parameters of the tuning fork gyro sensor.

$h_1$ (mm)	$h_2$ (mm)	$w$ (mm)	$\Delta n_{Rx}$ (rad/Nm)	$\Delta n_{Ry}$ (rad/Nm)	$\Delta m$ (kg)	$\Delta n_{Ra}$ (rad/Nm)	$\Delta n_{Rb}$ (rad/Nm)
0.5	1.5	3	25e-3	5.2e-3	32e-6	9e-3	2e-3
$\Delta n_{Rc}$ (rad/Nm)	$d_{33}$ (m/A)	$1/s_{33}^H$ (GPa)	$1/s_2$ (GPa)	$\mu_{r33}^S$	$\mu_{r33}^T$	$Y_r$ (A/Nm)	$N$ (turns)
5e-3	46e-9	210	70	100	500	576	500

#### 4. SUMMARY AND OUTLOOK

In this paper a new equivalent circuit of a magnetostrictive tuning fork gyro sensor including including a reversible Coriolis/centrifugal force transducer in a constant rotating frame of reference was developed and its behavior simulated with a circuit simulator. The network analysis supports the understanding and a forecast of the order of magnitude of the involved physical effects. The fact, that the model is restricted to constant rotating structures is no drawback for a lot of applications because the change of the angular velocity is often much slower than the dynamic vibrations of the structure. If needed, the angular velocity can be varied between single dynamic calculations.

#### ACKNOWLEDGEMENTS

This work was supported by ONR MURI Grant #N000140610530. The authors would like to thank also the Alexander von Humboldt Foundation for the support within the GAFOE follow up program.

#### REFERENCES

- [1] Bernstein, J., Cho, S., King, A.T., Kourepenis, A., Maciel, P., and M.Weinberg, "Micromachined comb-drive tuning fork rate gyroscope," Proc. IEEE Micro Electro Mechanical Systems, 143–148 (1993).
- [2] Satoh, A., Tomikawa, Y., and Ohnishi, K., "Piezoelectric vibratory gyro-sensor using a trident-type tuning fork resonator," Japanese Journal of Applied Physics, Part 1, 33(9B), 3217–3219 (1994).
- [3] Abe, H., Yoshida, T., and Turuga, K., "Piezoelectric-ceramic cylinder vibratory gyroscope," Japanese Journal of Applied Physics, Part 1, 31(9B), 3061–3063 (1992).
- [4] Putty, M.W., and Najafi, K., "A micromachined vibrating ring gyroscope," Proc. Solid-State Sensor and Actuator Workshop, 213–220 (1994).
- [5] Yoo, J.-H., Marschner, U., Flatau A. B., "Preliminary GALFENOL Vibratory Gyro-Sensor Design", Proc. SPIE 12th International Symposium on Smart Structures and Materials, Conference 5764 Smart Structures and Integrated Systems, 6-10 March, San Diego USA, 111-119 (2005).
- [6] Marschner, U.; Yoo, J.-H.; Starke, E.; Graham, F.; Mudivarathi, C.; Fischer, W.-J.; Flatau, A.B., "Electromechanical network modeling applied to magnetoelastic gyro sensor design," SPIE 7647, Sensors and Smart Structures Technologies for Civil, Mechanical, and Aerospace Systems 2010, 76472S (2010).
- [7] Gerlach and Dötzel, [Introduction to Microsystem Technology], John Wiley & Sons, (2008).
- [8] Starke, E. and Marschner, U., "Lumped Circuit Model for Gyro Sensors Incorporating Coriolis and Centrifugal Force", EUROSENSORS 2014, the 28th European Conference on Solid-State Transducers, Procedia Engineering, Vol. 87, 432-435 (2014)
- [9] Lenk, A., Ballas, R.G., Werthschützky R. and Pfeifer, G. [Electromechanical Systems in Microtechnology and Mechatronics], Springer (2010).
- [10] Marschner, U., Gerlach, G., Starke, E., Lenk, A.: "Equivalent circuit models of two-layer flexure beams with excitation by temperature, humidity, pressure, piezoelectric or piezomagnetic interactions," Journal of Sensors and Sensor Systems 3, (2), 187–211, (2014).